

Growing Crystalline Chalcogenidoarsenates in Surfactants: From Zero-Dimensional Cluster to Three-Dimensional Framework

Wei-Wei Xiong,^{†,§} Eashwer Umesh Athresh,^{†,§} Yu Ting Ng,[†] Junfeng Ding,[‡] Tom Wu,[‡] and Qichun Zhang^{*,†}

[†]School of Materials Science and Engineering, Nanyang Technological University, Singapore 639798, Singapore

[‡]Division of Physics and Applied Physics, School of Physical and Mathematical Sciences, Nanyang Technological University, Singapore 637371, Singapore

S Supporting Information

ABSTRACT: Although surfactants have been widely used to tailor the size, shape, and surface properties of nanocrystals and control the pore size and phases of mesoporous frameworks, the use of surfactants as reaction media to grow chalcogenide crystals is unprecedented. In addition, compared with ionic liquids, surfactants are much cheaper and can have multifunctional properties such as acidic, basic, neutral, cationic, anionic, or even block. These features suggest that surfactants could be promising reaction platforms for the development of novel chalcogenide crystals. In this work, we used chalcogenidoarsenates as a model system to demonstrate our strategy. By using three different surfactants as reaction media, we obtained a series of novel thioarsenates ranging from a zero-dimensional (0D) cluster to a three-dimensional (3D) framework, namely, $[\text{NH}_4]_8[\text{Mn}_2\text{As}_4\text{S}_{16}]$ (**1**), $[\text{Mn}(\text{NH}_3)_6][\text{Mn}_2\text{As}_2\text{S}_8(\text{N}_2\text{H}_4)_2]$ (**2**), $[\text{enH}][\text{Cu}_3\text{As}_2\text{S}_5]$ (**3**), and $[\text{NH}_4][\text{MnAs}_3\text{S}_6]$ (**4**). The band gaps (estimated from the steep absorption edges) were found to be 2.31 eV for **1** (0D), 2.46 eV for **2** (1D), 1.91 eV for **3** (2D), and 2.08 eV for **4** (3D). The magnetic study of **4** indicated weak antiferromagnetic behavior. Our strategy of growing crystalline materials in surfactants could offer exciting opportunities for preparing novel crystalline materials with diverse structures and interesting properties.

New strategies for growing crystalline chalcogenides are of importance in both fundamental sciences and technological applications. Currently, the growth of chalcogenide crystals is mainly performed using high-temperature solid-state reactions, hydrothermal and solvothermal conditions, or room-temperature processes.^{1,2} Very recently, ionic liquids have become important reaction media for the synthesis of new chalcogenide compounds because of their unusual properties such as high thermal/chemical stability, wide liquid-phase range, and low vapor pressure.^{2d,3} However, their expensive prices and the limited number of commercially available sources have posed a limitation on the use of ionic liquids in producing new chalcogenide materials. This unfortunate situation motivated us to develop a novel alternative strategy: growing crystalline chalcogenides in surfactants.

Although surfactants have been widely used to control the growth of colloidal inorganic nanocrystals and porous frame-

works,⁴ the use of surfactants as solvents to grow chalcogenide crystals has remained unexplored. It is well-known that surfactants can not only tailor the sizes, shapes, and surface properties of nanocrystals but also control the pore sizes and phases of mesoporous frameworks. These advantages convinced us that the diverse structures of crystalline chalcogenides could be achieved if we were to employ surfactants as the reaction media. In addition, compared with ionic liquids, surfactants are much cheaper and can have multifunctional properties such as acidic, basic, neutral, cationic, anionic, or even block. These features should offer more choices for controlling the crystal growth.

In this context, we used chalcogenidoarsenates as a model system to demonstrate our strategy because of their variable structural factors and interesting properties such as magnetism, fluorescence, nonlinear optics, and conductivity.⁵ Typically, there are two kinds of primary building units in chalcogenidoarsenates: trigonal-pyramidal $[\text{AsQ}_3]^{3-}$ and tetrahedral $[\text{AsQ}_4]^{3-}$ (Q = S, Se). When two building units are condensed or combined with main-group, transition, or rare-earth metals under solvothermal or molten salt conditions, various structures are produced.⁶ If these reactions could be performed in surfactants, more new structures with diverse properties would be anticipated because the surfactant would have strong interactions with the crystal faces during crystal growth. This prediction has been proved by our recent explorations on applying various surfactants as solvent media in the preparation of crystalline metal chalcogenides. Here we report on the first application of surfactants as reaction media in the synthesis of metal chalcogenidoarsenates.

The choice of surfactants in this research was based on the melting point (liquid, low or high melting point), the charge state (charged or neutral), and the ability to coordinate with metals. On the basis of these factors, three different surfactants were selected for use as solvents (Figure 1): poly(vinylpyrrolidone) (PVP), poly(ethylene glycol)-400 (PEG-400), and 1-hexadecyl-3-methylimidazolium chloride ($[\text{Hmim}]\text{-Cl}$). In our continuous research, we have found that other surfactants also work very well, and these results are still under investigation. By using these three different surfactants, we obtained a series of novel thioarsenates ranging from a zero-

Received: November 28, 2012

Published: January 11, 2013



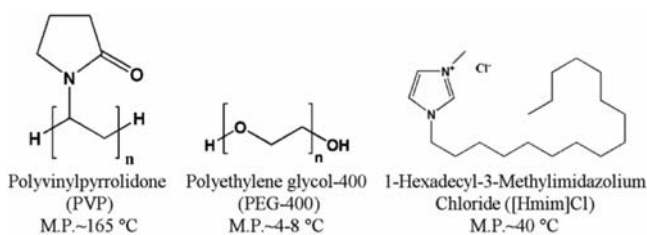


Figure 1. Three different surfactants used in synthesizing crystalline thioarsenates.

dimensional (0D) cluster to a three-dimensional (3D) framework, namely, $[\text{NH}_4]_8[\text{Mn}_2\text{As}_4\text{S}_{16}]$ (**1**, 0D), $[\text{Mn}(\text{NH}_3)_6][\text{Mn}_2\text{As}_2\text{S}_8(\text{N}_2\text{H}_4)_2]_n$ (**2**, 1D), $[\text{enH}][\text{Cu}_3\text{As}_2\text{S}_5]_n$ (**3**, 2D), and $[\text{NH}_4][\text{MnAs}_3\text{S}_6]_n$ (**4**, 3D). It is noteworthy that when the surfactant was removed, either no crystals (for **1**, **2**, and **4**) or a small amount (less than 3% yield) of crystals (for **3**) was obtained. This approach demonstrates the potential of surfactants as reaction media for the preparation of a wide range of novel crystalline chalcogenides.

When PVP was used as the solvent medium, yellow block crystals of **1** ($\text{H}_{32}\text{N}_8\text{Mn}_2\text{As}_4\text{S}_{16}$) were obtained when Mn, As_2S_3 , S, and $\text{N}_2\text{H}_4 \cdot \text{H}_2\text{O}$ were mixed in a 1:1:2.5:8 molar ratio and heated at 160 °C for 5 days. Single-crystal X-ray analysis revealed that **1** crystallizes in the space group $P2_1/n$.⁷ The structure contains discrete $[\text{Mn}_2\text{As}_4\text{S}_{16}]^{8-}$ clusters and NH_4^+ cations that are generated from the decomposition of hydrazine (Figure 2a). The asymmetric unit of **1** contains two crystallographically independent As^{5+} ions, one Mn^{2+} ion,

eight S^{2-} ions, and four NH_4^+ cations. Each As^{5+} ion coordinates with four S^{2-} anions to form an $[\text{AsS}_4]$ tetrahedron, while each Mn^{2+} ion adopts a slightly distorted octahedral coordination geometry by bonding to six S^{2-} ions. Two $[(\text{As}1)\text{S}_4]$ tetrahedrons connect with two Mn1 ions to form a tetranuclear trans double-semicube $[\text{Mn}_2\text{As}_2\text{S}_8]$ cluster, which is further coordinated by two $[(\text{As}2)\text{S}_4]$ tetrahedrons to form a discrete $[\text{Mn}_2\text{As}_4\text{S}_{16}]^{8-}$ cluster. The NH_4^+ counteranions reside in the spaces between the discrete anionic $[\text{Mn}_2\text{As}_4\text{S}_{16}]^{8-}$ clusters. The As–S and Mn–S bond lengths are in the ranges 2.1433(5)–2.1894(5) and 2.5863(6)–2.7565(6) Å, respectively. It should be noted that **1** is isostructural with the known molecular thioarsenate complexes $\text{A}_8[\text{Mn}_2(\text{AsS}_4)_4]$ (A = K, Rb, Cs).⁸

When PVP was replaced with PEG-400 and the same starting materials as used to prepare **1** were heated at 110 °C for 5 days, light-yellow plate crystals of **2** were obtained. Compound **2** belongs to the space group $C2/c$ and features anionic one-dimensional (1D) $[\text{Mn}_2\text{As}_2\text{S}_8(\text{N}_2\text{H}_4)_2]_n^{2n-}$ chains parallel to the *b* axis (Figure 2b).⁷ The asymmetric unit of **2** consists of one crystallographically independent As^{5+} ion, one and a half Mn^{2+} ions (one Mn ion is located at a special position with C_2 symmetry), four S^{2-} ions, three NH_3 molecules, and one $\text{H}_2\text{N}-\text{NH}_2$ molecule. Both the Mn1 and Mn2 ions adopt slightly distorted octahedral geometries; the Mn1 ions are coordinated with four S atoms and two N atoms from two different hydrazine ligands, and the Mn2 ions are coordinated with six NH_3 molecules to form $[\text{Mn}(\text{NH}_3)_6]^{2+}$ complexes that act as charge-balancing species. Pairs of $[(\text{As}1)\text{S}_4]$ tetrahedrons

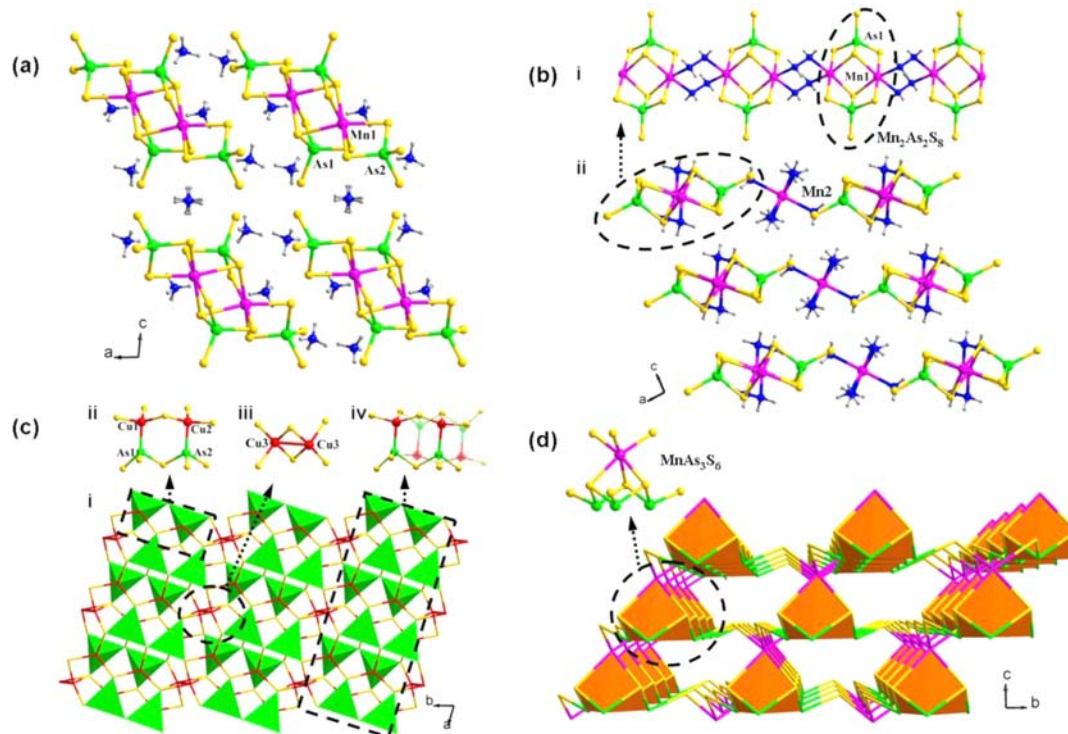


Figure 2. (a) View of the discrete $[\text{Mn}_2\text{As}_4\text{S}_{16}]^{8-}$ clusters in **1** packed along the *b* axis. (b) (i) One-dimensional anionic $[\text{Mn}_2\text{As}_2\text{S}_8(\text{N}_2\text{H}_4)_2]_n^{2n-}$ chain in **2** built up by connecting tetranuclear $[\text{Mn}_2\text{As}_2\text{S}_8]$ trans double semicubes with pairs of $\text{H}_2\text{N}-\text{NH}_2$ molecules and (ii) view of the packing of these chains along the *b* axis separated by $[\text{Mn}(\text{NH}_3)_6]^{2+}$ cations. (c) (i) Single anionic $[\text{Cu}_3\text{As}_2\text{S}_5]_n^{n-}$ layer in **3** viewed along the *c* axis. The $[\text{CuAsS}_6]$ dimers (ii) are connected to each other via vertex-sharing (iv) to form infinite $[\text{Cu}_2\text{As}_2\text{S}_{10}]_n^{n-}$ ribbons parallel to the *a* axis, with $[\text{CuAsS}_6]$ units in adjacent ribbons being further linked by interconnected pairs of $[(\text{Cu}3)\text{S}_4]$ tetrahedra (iii). (d) Three-dimensional framework in **4** constructed from $[\text{MnAs}_3\text{S}_6]$ semicubes, viewed along the *a* axis.

connect with pairs of Mn1 ions to form tetranuclear $[\text{Mn}_2\text{As}_2\text{S}_8]$ trans double semicubes, which are also observed in **1**. It should be noted that in the structure of **1**, the two Mn1 ions in each $[\text{Mn}_2\text{As}_2\text{S}_8]$ cluster connect with two $[(\text{As}_2)\text{S}_4]$ tetrahedrons to form a discrete $[\text{Mn}_2\text{As}_4\text{S}_{16}]^{8-}$ cluster, while in the structure of **2**, Mn1 atoms in neighboring $[\text{Mn}_2\text{As}_2\text{S}_8]$ clusters are bridged by two $\text{H}_2\text{N}-\text{NH}_2$ ligands to yield anionic 1D $[\text{Mn}_2\text{As}_2\text{S}_8(\text{N}_2\text{H}_4)_2]^{2n-}$ chains oriented along the *b* axis [Figure 2b(i)]. The isolated $[\text{Mn}(\text{NH}_3)_6]^{2+}$ cations act as charge-balancing units and fill in the spaces between the anionic $[\text{Mn}_2\text{As}_2\text{S}_8(\text{N}_2\text{H}_4)_2]^{2n-}$ chains. The As–S bond lengths range from 2.1234(9) to 2.1899(10) Å, and the Mn–S and Mn–N bond lengths fall in the ranges 2.6096(12)–2.6699(10) and 2.255(3)–2.296(3) Å, respectively.

Dark-red flake crystals of **3** were obtained by heating a mixture of CuI, As_2S_3 , S, and ethylenediamine (en) in a 1:0.5:2.5:7.5 molar ratio using PEG-400 as the solvent at 160 °C for 5 days. Compound **3** belongs to the space group $P\bar{1}$, and its structure features two-dimensional (2D) anionic $[\text{Cu}_3\text{As}_2\text{S}_5]^{n-}$ layers [Figure 2c(i)] separated by protonated en cations (enH^+).⁷ The asymmetric unit of **3** is made up of two crystallographically independent As^{3+} ions, three Cu^{3+} ions, five S^{2-} ions, and enH^+ cation. Each As1 and As2 is coordinated with three S atoms and one Cu atom to form a $[\text{AsCuS}_3]$ tetrahedron, while each Cu1 and Cu2 is surrounded by three S atoms and one As atom to generate an inverted $[\text{CuAsS}_3]$ tetrahedra. Each $[\text{AsCuS}_3]$ group combines with a $[\text{CuAsS}_3]$ unit to form a dumbbell-like $[\text{CuAsS}_6]$ dimer [Figure 2c(ii)]. Interestingly, each Cu3 is coordinated with four S atoms from adjacent $[\text{CuAsS}_6]$ dimers to form a $[(\text{Cu}3)\text{S}_4]$ tetrahedron, and pairs of these tetrahedra are connected to each other through edge sharing with a Cu–Cu bond length of 2.672(6) Å [Figure 2c(iii)]. The adjacent $[\text{CuAsS}_6]$ dimers are alternately arranged by vertex sharing to form infinite $[\text{Cu}_2\text{As}_2\text{S}_{10}]$ ribbons along oriented along the *a* axis [Figure 2c(iv)], which are linked via Cu3–Cu3 and Cu2–S5 bonding to yield anionic $[\text{Cu}_3\text{As}_2\text{S}_5]^{n-}$ layers. The As–S, Cu–S, and Cu–As bond lengths fall in the ranges 2.216(5)–2.346(5), 2.255(5)–2.476(6), and 2.450(3)–2.514(3) Å, respectively, which are comparable with those reported in the literature.⁹ The anionic $[\text{Cu}_3\text{As}_2\text{S}_5]^{n-}$ layers in **3** are isostructural with the formerly reported $[\text{Cu}_3\text{Sb}_2\text{S}_5]^{n-}$ layers based on Cu–Sb–S composition.¹⁰

When $[\text{Hmim}]\text{Cl}$ surfactant was employed as the solvent and the same starting materials as for **1** were heated at 140 °C for 5 days, red block crystals of **4** were obtained. Compound **4** crystallizes in the space group $R\bar{3}$.⁷ Its structure features a 3D anionic $[\text{MnAs}_3\text{S}_6]^{n-}$ framework with channels filled by NH_4^+ cations generated from the decomposition of hydrazine (Figure 2d). The asymmetric unit of **4** is made up of one crystallographically independent As^{3+} ion, one-third of a Mn^{2+} ion with C_3 symmetry, two S^{2-} ions, and one-third of an NH_4^+ cation. The As atom is coordinated with three S atoms to form a trigonal pyramid, with As–S bond lengths ranging from 2.1773(6) to 2.3202(5) Å. The Mn^{2+} ion is coordinated with six S atoms to form a slightly distorted octahedron with Mn–S bond lengths in the range 2.5193(6)–2.7237(6) Å. Through S··S edge sharing, three AsS_3 trigonal pyramids connect with one MnS_6 octahedron to generate a $[\text{MnAs}_3\text{S}_6]$ semicube, which is further coordinated with the adjacent six semicubes via six S atoms to form a 3D framework.

The solid-state UV–vis diffuse-reflectance spectra of **1–4** were measured at room temperature and converted to optical

absorption data using the Kubelka–Munk function.¹¹ As shown in Figure 3, the band gaps can be estimated from the steep

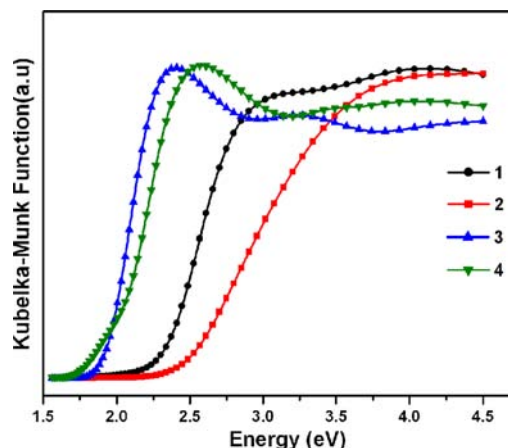


Figure 3. Solid-state optical absorption spectra of **1–4**.

absorption edges as 2.31 eV for **1**, 2.46 eV for **2**, 1.91 eV for **3**, and 2.08 eV for **4**, which are consistent with their colors. The band gap of **1** is comparable to those of the isostructural molecular thioarsenate complexes $\text{A}_8[\text{Mn}_2(\text{AsS}_4)_4]$ (A = K, Rb, Cs) (2.25–2.33 eV).⁸ The steep absorption edges of compounds **1–4** may be attributed to charge transfer from the sulfur-based valence band to the mainly transition-metal-based conduction band.

The thermal stabilities of **1–4** were measured by thermogravimetric analysis (TGA) from 25 to 500 °C under a N_2 atmosphere (Figure S1 in the Supporting Information). The TGA curve of **1** exhibits two distinct stages with weight losses of 24.0 and 20.6%, corresponding to the loss per formula unit of eight NH_3 molecules (12.8%) and three H_2S molecules (9.6%) in the first stage and one As_2S_2 molecule (20.0%) in the second stage. Compound **2** displays one main weight loss step of 65.1%, which is attributed to the loss of six NH_3 molecules (13.8%), two H_2NNH_2 molecules (8.7%), three S molecules (13%), and one As_2S_2 molecule (29.0%) per formula unit. In the case of **3**, two distinct stages with weight losses of 17.8 and 15.5% were observed, corresponding to the loss per formula unit of one ethylenediamine molecule (10.7%) and one S molecule (5.7%) in the first stage and three S molecules (17.1%) in the second stage. Compound **4** undergoes a main weight loss of 77.9% due to the loss of one NH_3 molecule (3.5%), one and a half As_2S_2 molecules (65.5%), and one S molecule (6.5%) per formula unit.

The magnetic susceptibility (χ_M) of **4** was measured over the temperature range 5–300 K. As shown in the Figure 4 inset, the plot of $1/\chi_M$ versus *T* obeys the Curie–Weiss law over the whole temperature range. From the Curie–Weiss equation $\chi_M = C/(T - \theta)$, the value of the Curie constant (*C*) and the Weiss constant (θ) were obtained as 4.12 emu K/mol and –5.9 K, respectively, indicating a weak antiferromagnetic interaction between the magnetic Mn^{2+} ions (the distance between nearest Mn^{2+} ions is 6.42 Å). The effective magnetic moment (μ_{eff}) per Mn^{2+} ion in **4** is $5.68\mu_B$, which is close to the value of $5.92\mu_B$ for a free Mn^{2+} ion.¹²

In conclusion, we have opened up a new route for preparing crystalline chalcogenides by employing various surfactants as reaction media. For the first time, a series of thioarsenates ranging from a zero-dimensional cluster to a three-dimensional

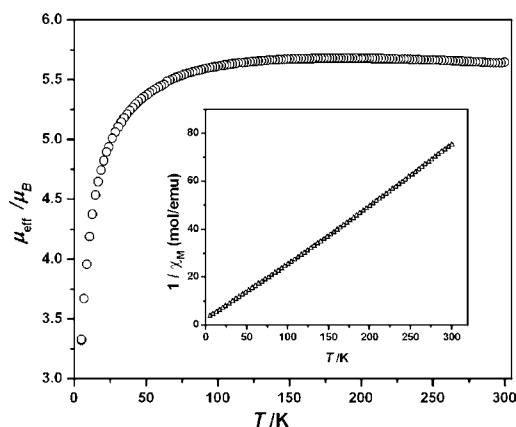


Figure 4. Plots of the effective magnetic moment (μ_{eff}) and (inset) the reciprocal of the magnetic susceptibility ($1/\chi_M$) vs temperature (T) for 4.

framework have been synthesized in surfactant environments (PVP, PEG-400, and [Hmim]Cl) by using amines as templates. Our results confirmed that surfactants can effectively control crystal growth. We believe that this new synthetic strategy offers exciting opportunities for synthesizing novel crystalline materials with diverse structures and interesting properties.

■ ASSOCIATED CONTENT

● Supporting Information

Experimental details, TGA curves, energy-dispersive X-ray spectra, powder X-ray diffraction patterns, and crystallographic data (CIF). This material is available free of charge via the Internet at <http://pubs.acs.org>.

■ AUTHOR INFORMATION

Corresponding Author

qczhang@ntu.edu.sg

Author Contributions

[§]W.-W.X. and E.U.A. contributed equally.

Notes

The authors declare no competing financial interest.

■ ACKNOWLEDGMENTS

Q.Z. acknowledges the financial support from AcRF Tier 1 (RG 18/09) and Tier 2 (ARC 20/12) from MOE, the CREATE Program (Nanomaterials for Energy and Water Management) from NRF, and the New Initiative Fund from NTU, Singapore.

■ REFERENCES

- (1) (a) Krebs, B. *Angew. Chem., Int. Ed. Engl.* **1983**, *22*, 113. (b) Kanatzidis, M. G.; Huang, S. P. *Coord. Chem. Rev.* **1994**, *130*, 509. (c) Sheldrick, W. S.; Wachhold, M. *Angew. Chem., Int. Ed. Engl.* **1997**, *36*, 207. (d) Zhang, Q.; Bu, X.; Zhang, J.; Wu, T.; Feng, P. *J. Am. Chem. Soc.* **2007**, *129*, 8412. (e) Zhang, Q.; Bu, X.; Lin, Z.; Feng, P. *Chem. Mater.* **2008**, *20*, 3239. (f) Zhang, Q.; Malliakas, C. D.; Kanatzidis, M. G. *Inorg. Chem.* **2009**, *48*, 10910. (g) Zhang, Q.; Armatas, G.; Kanatzidis, M. G. *Inorg. Chem.* **2009**, *48*, 8665. (h) Liu, Y.; Wei, F.; Yeo, S. N.; Lee, F. M.; Kloc, C.; Yan, Q.; Hng, H. H.; Ma, J.; Zhang, Q. *Inorg. Chem.* **2012**, *51*, 4414.
- (2) (a) Feng, P. Y.; Bu, X. H.; Zheng, N. F. *Acc. Chem. Res.* **2005**, *38*, 293. (b) Dehnen, S.; Melullis, M. *Coord. Chem. Rev.* **2007**, *251*, 1259. (c) Zhou, J.; Dai, J.; Bian, G. Q.; Li, C. Y. *Coord. Chem. Rev.* **2009**, *253*, 1221. (d) Zhang, Q.; Chung, I.; Jang, J. I.; Ketterson, J. B.; Kanatzidis, M. G. *J. Am. Chem. Soc.* **2009**, *131*, 9896. (e) Zhang, Q.; Chung, I.

Jang, J. I.; Ketterson, J. B.; Kanatzidis, M. G. *Chem. Mater.* **2009**, *21*, 12. (f) Vaqueiro, P. *Dalton Trans.* **2010**, *39*, 5965.

(3) (a) Biswas, K.; Zhang, Q.; Chung, I.; Song, J. H.; Androulakis, J.; Freeman, A. J.; Kanatzidis, M. G. *J. Am. Chem. Soc.* **2010**, *132*, 14760. (b) Ahmed, E.; Isaeva, A.; Fiedler, A.; Haft, M.; Ruck, M. *Chem.—Eur. J.* **2011**, *17*, 6847. (c) Freudenmann, D.; Feldmann, C. *Dalton Trans.* **2011**, *40*, 452. (d) Li, J. R.; Xie, Z. L.; He, X. W.; Li, L. H.; Huang, X. Y. *Angew. Chem., Int. Ed.* **2011**, *50*, 11395. (e) Lin, Y. M.; Massa, W.; Dehnen, S. *J. Am. Chem. Soc.* **2012**, *134*, 4497. (f) Xiong, W. W.; Li, J. R.; Hu, B.; Tan, B.; Li, R. F.; Huang, X. Y. *Chem. Sci.* **2012**, *3*, 1200. (g) Ahmed, E.; Beck, J.; Daniels, J.; Doert, T.; Eck, S. J.; Heerwig, A.; Isaeva, A.; Lidin, S.; Ruck, M.; Schnelle, W.; Stankowski, A. *Angew. Chem., Int. Ed.* **2012**, *51*, 8106.

(4) (a) Yin, Y.; Alivisatos, A. P. *Nature* **2005**, *437*, 664. (b) Xia, Y.; Yang, P.; Sun, Y.; Wu, Y.; Mayers, B.; Gates, B.; Yin, Y.; Kim, F.; Yan, H. *Adv. Mater.* **2003**, *15*, 353.

(5) (a) Drake, G. W.; Kolis, J. W. *Coord. Chem. Rev.* **1994**, *137*, 131. (b) Sheldrick, W. S.; Wachhold, M. *Coord. Chem. Rev.* **1998**, *176*, 211. (c) Fu, M. L.; Guo, G. C.; Cai, L. Z.; Zhang, Z. J.; Huang, J. S. *Inorg. Chem.* **2005**, *44*, 184. (d) Wang, J. Z.; Lin, M.; Zhang, T. Y.; Yan, Y. L.; Ho, P. C.; Xu, Q. H.; Loh, K. P. *J. Am. Chem. Soc.* **2008**, *130*, 11596. (e) Bera, T. K.; Jang, J. I.; Ketterson, J. B.; Kanatzidis, M. G. *J. Am. Chem. Soc.* **2009**, *131*, 75. (f) Bera, T. K.; Song, J. H.; Freeman, A. J.; Jang, J. I.; Ketterson, J. B.; Kanatzidis, M. G. *Angew. Chem., Int. Ed.* **2008**, *47*, 7828. (g) Bera, T. K.; Jang, J. I.; Song, J. H.; Malliakas, C. D.; Freeman, A. J.; Ketterson, J. B.; Kanatzidis, M. G. *J. Am. Chem. Soc.* **2010**, *132*, 3484.

(6) (a) Chou, J. H.; Kanatzidis, M. G. *Inorg. Chem.* **1994**, *33*, 5372. (b) Chou, J. H.; Kanatzidis, M. G. *Chem. Mater.* **1995**, *7*, 5. (c) Wood, P. T.; Schimek, G. L.; Kolis, J. W. *Chem. Mater.* **1996**, *8*, 721. (d) Iyer, R. G.; Do, J.; Kanatzidis, M. G. *Inorg. Chem.* **2003**, *42*, 1475. (e) Fu, M. L.; Guo, G. C.; Liu, X.; Chen, W. T.; Liu, B.; Huang, J. S. *Inorg. Chem.* **2006**, *45*, 5793. (f) Bera, T. K.; Kanatzidis, M. G. *Inorg. Chem.* **2008**, *47*, 7068. (g) Kromm, A.; Sheldrick, W. S. *Z. Anorg. Allg. Chem.* **2008**, *634*, 2948. (h) Wang, Z. Q.; Zhang, H. J.; Wang, C. *Inorg. Chem.* **2009**, *48*, 8180. (i) Wu, Y. D.; Bensch, W. *Inorg. Chem.* **2009**, *48*, 2729. (j) Jia, D. X.; Zhao, J.; Pan, Y. L.; Tang, W. W.; Wu, B.; Zhang, Y. *Inorg. Chem.* **2011**, *50*, 7195. (k) Liu, G. N.; Jiang, X. M.; Wu, M. F.; Wang, G. E.; Guo, G. C.; Huang, J. S. *Inorg. Chem.* **2011**, *50*, 5740. (l) Du, K. Z.; Feng, M. L.; Li, J. R.; Huang, X. Y. *CrystEngComm* **2012**, *14*, 4959.

(7) Crystal data for 1: $\text{H}_{32}\text{N}_8\text{Mn}_2\text{As}_4\text{S}_{16}$, $M = 1067.02$, monoclinic, $P2_1/n$, $a = 9.2086(4)$ Å, $b = 8.8211(4)$ Å, $c = 20.7793(10)$ Å, $\beta = 96.047(2)^\circ$, $V = 1678.51(13)$ Å³, $Z = 2$, $T = 103(2)$ K, $R_1 = 0.0210$ and $wR_2 = 0.0427$ for $I > 2\sigma(I)$, GOF = 1.052. Crystal data for 2: $\text{H}_{26}\text{N}_{10}\text{Mn}_3\text{As}_2\text{S}_8$, $M = 737.53$, monoclinic, $C2/c$, $a = 24.312(5)$ Å, $b = 7.9301(16)$ Å, $c = 12.412(3)$ Å, $\beta = 93.21(3)^\circ$, $V = 2389.2(9)$ Å³, $Z = 4$, $T = 153(2)$ K, $R_1 = 0.0247$ and $wR_2 = 0.0626$ for $I > 2\sigma(I)$, GOF = 1.001. Crystal data for 3: $\text{C}_2\text{H}_9\text{N}_2\text{Cu}_3\text{As}_2\text{S}_5$, $M = 561.91$, triclinic, $P\bar{1}$, $a = 6.166(2)$ Å, $b = 9.604(4)$ Å, $c = 10.790(4)$ Å, $\alpha = 78.118(6)^\circ$, $\beta = 77.984(6)^\circ$, $\gamma = 71.816(5)^\circ$, $V = 586.9(4)$ Å³, $Z = 2$, $T = 296(2)$ K, $R_1 = 0.0850$ and $wR_2 = 0.2719$ for $I > 2\sigma(I)$, GOF = 1.004. Crystal data for 4: $\text{H}_4\text{NMnAs}_3\text{S}_6$, $M = 490.10$, trigonal, $R\bar{3}$, $a = 9.1872(4)$ Å, $c = 10.8539(5)$ Å, $V = 793.38(6)$ Å³, $Z = 3$, $T = 93(2)$ K, $R_1 = 0.0192$ and $wR_2 = 0.0396$ for $I > 2\sigma(I)$, GOF = 0.929.

(8) Iyer, R. G.; Kanatzidis, M. G. *Inorg. Chem.* **2004**, *43*, 3656.

(9) (a) Jerome, J. E.; Wood, P. T.; Pennington, W. T.; Kolis, J. W. *Inorg. Chem.* **1994**, *33*, 1733. (b) Hanko, J. A.; Chou, J. H.; Kanatzidis, M. G. *Inorg. Chem.* **1998**, *37*, 1670.

(10) Spetzler, V.; Nather, C.; Bensch, W. *Inorg. Chem.* **2005**, *44*, 5805.

(11) Wendlandt, W. M.; Hecht, H. G. *Reflectance Spectroscopy*; Interscience: New York, 1966.

(12) Van Vleck, J. H. *The Theory of Electric and Magnetic Susceptibilities*; Oxford University: Oxford, U.K., 1932.